Title: Arctic defaunation initiated a cascade of mammal–plant interaction shifts through dispersal dynamics

Authors:

Sisi Liu[1]*, Kathleen R. Stoof-Leichsenring[1], Marc-Thorsten Hütt[2], Weihan Jia[1], Boris K. Biskaborn[1], Bernhard Diekmann[1], Darrell S. Kaufman[3], Hanno Meyer[1], Martin Melles[4], Luidmila A. Pestryakova[5], Ulrike Herzschuh[1,6,7]*

Affiliations:

[1]Polar Terrestrial Environmental Systems, Alfred Wegener Institute Helmholtz Centre for Polar and Marine Research, Potsdam, 14473, Germany

[2]Computational Systems Biology, Constructor University, Bremen, 28759, Germany

[3]School of Earth and Sustainability, Northern Arizona University, Arizona, 86011, USA

[4]Institute of Geology and Mineralogy, University of Cologne, Cologne, 50674, Germany

[5]Institute of Natural Sciences, North-Eastern Federal University of Yakutsk, Yakutsk, 677007, Russia

[6]Institute of Environmental Science and Geography, University of Potsdam, Potsdam, 14476, Germany

[7]Institute of Biochemistry and Biology, University of Potsdam, Potsdam, 14476, Germany

*Corresponding authors:

Sisi Liu (sisi.liu@awi.de); Ulrike Herzschuh (Ulrike.Herzschuh@awi.de)

Abstract: Amid accelerating defaunation, it remains unclear whether the loss of large mammals can trigger ecosystem collapse and through which functional pathways. Using sedimentary ancient metagenomics, we reveal the overlooked role of large mammal defaunation in driving the collapse of the glacial mammoth-steppe. Network analyses identified rewiring of mammal interactions during the late glacial triggering cascading effects. Crucially, megafaunal-mediated long-distance seed dispersal buffered vegetation turnover during periods of rapid climate warming but weakened with consecutive losses of vital dispersal interactions leading to the steppe–tundra's transition to open woodland in the early Holocene. Trophic interactions could not prevent turnover and became more dominant afterwards with the more stable climate. We identified resilient interactions that may support recovery, demonstrating the potential of rewilding to restore Arctic ecosystems.

Main Text

Introduction

Climate change is accelerating global declines, extinctions, and local extirpations of terrestrial animals (*1*), with large-bodied mammals—particularly herbivores and predators—being most at risk (*2*). The extent to which these declines disrupt trophic (e.g., predation, herbivory) and mutualistic (e.g., seed dispersal) interactions, and how such disruptions unfold over time, remains insufficiently understood (*3*, *4*). Yet defaunation is not a uniquely contemporary phenomenon (*5*). A similar pronounced event happened around the end of the last glacial period (*6*), when many large-bodied mammals like mammoths disappeared. This was concurrent with the collapse of the vast mammoth-steppe ecosystem (*7*), once the largest biome on Earth.

While drivers of megafaunal extinction have been debated for decades, the ecological consequences, particularly the collapse of biotic interactions, are only beginning to be understood (*8*). Crucially, Holarctic megafaunal declines unfolded gradually (*6*), likely altering terrestrial ecosystems well before final extinction (*9*). This raises the hypothesis—so far untested in paleoecology—that cascading losses of biotic interactions due to defaunation may have contributed to the ecological reorganization of the mammoth-steppe ecosystem.

Alternative to biotic interaction loss, the role of defaunation in enabling the emergence of novel interactions has received even less attention (*10*, *11*). Different types of reconstructed interaction networks offer complementary insights: for example, predator-prey webs suggest greater functional redundancy in the Pleistocene than Holocene, with release from top-predator loss leading to increases in megaherbivore density and distribution (*12*). Herbivory-plant interactions indicate that some surviving small-bodied herbivores shifted from browsing to mixed feeding between the Pleistocene and Holocene (*13*), potentially forming new trophic interactions. Plant–frugivore seed dispersal interactions exhibited profound rearrangement rather than complete structural collapse after late Pleistocene megafaunal loss (*10*). While this suggests a degree of functional replacement, it raises open questions about whether such interaction rewiring may have influenced the composition of plant communities.

Additionally, the mechanisms behind the re-establishment of lost interactions, so-called "resilient links", are still not well understood. Clarifying the role of functional traits in this process could provide important insights for coextinction risk assessments, particularly by accounting for interaction rewiring, the ability of a taxon to switch partners in response to perturbations as a potential buffer against cascading extinctions (*14*).

While much has been learned about past changes in taxonomic abundance across space and time, the dynamics of ecological interactions remain underexplored, as interactions are rarely preserved due to the sparse fossil record. Sedimentary ancient DNA (sedaDNA) holds promise to infer biotic interactions by providing spatially and temporally extensive evidence of past taxonomic co-occurrence. When combined with species traits, sedaDNA can help infer potential ecological interaction pathways with greater resolution than fossil records and more empirical grounding than trait-matching models alone.

To address these knowledge gaps, we conducted ancient metagenomic (shotgun sequencing) analyses of terrestrial mammals and plants from 119 lake sediment samples across Siberia and the North American Arctic spanning the past 25,000 years (Fig. 1A). These samples, collected from six lake cores located in regions that overlap with known megafaunal fossil distributions, provide the spatial and temporal resolution necessary to track changes in size-selective

mammalian defaunation such as the woolly mammoth and associated plant community dynamics and their interaction networks.

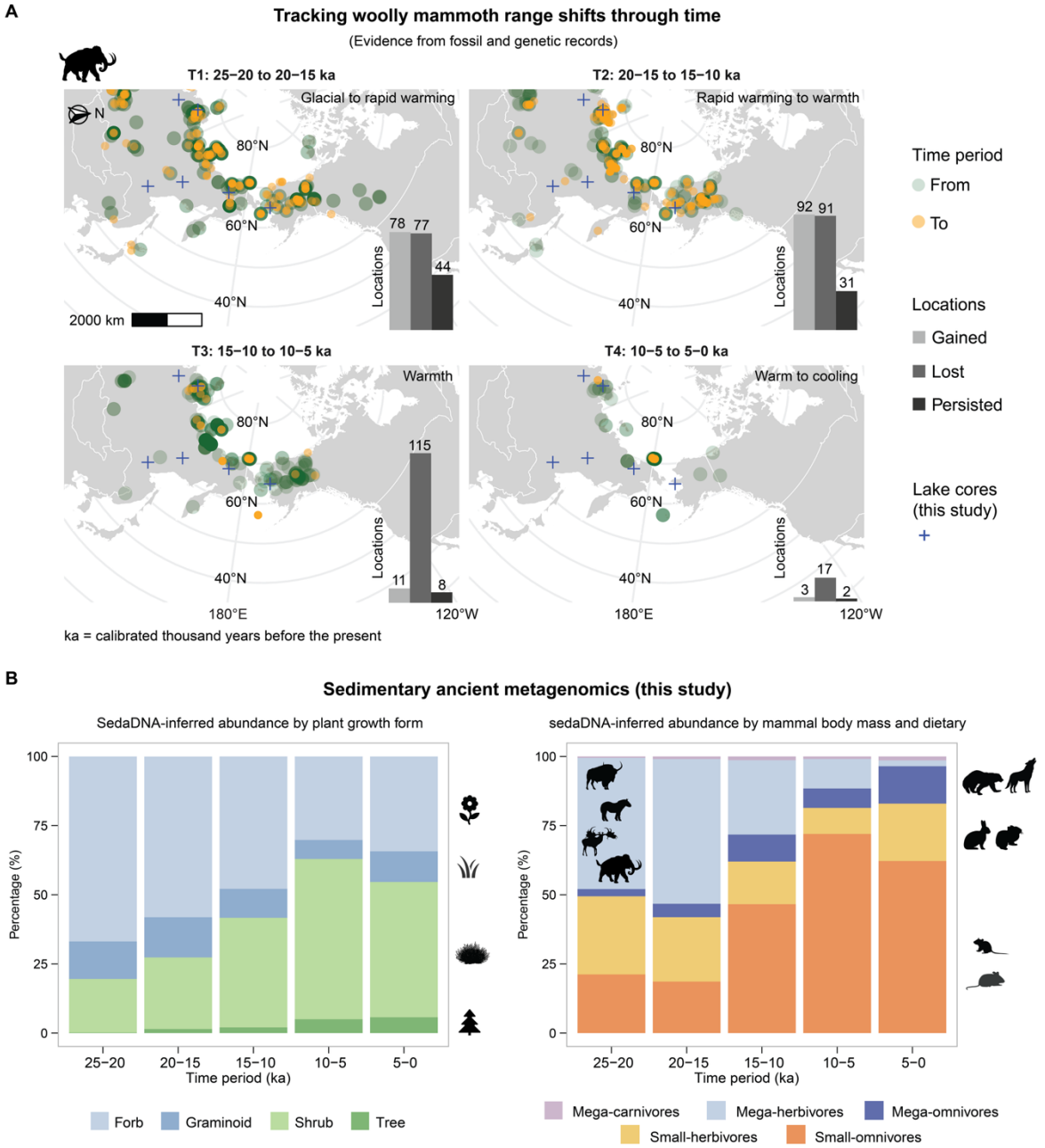

Fig. 1 Evidence of community changes in northern Eurasia and North America over the past 25 ka. (**A**) Illustration of woolly mammoth range changes across four time transitions based on fossil and genetic records, showing progressive expansion and contraction of its geographical distribution, broadly reflecting population trends across cold and warm climatic phases, culminating in extinction during the late Holocene (5–0 ka) (*7*, *15*, *16*). Locations of studied lake sediment cores are indicated. Fossil and genetic records are colored by time, with green for earlier periods ("from") and orange for later ones ("to"). The dot size helps visualize overlapping locations. (**B**) In this study, sedaDNA-inferred vegetation shifts from steppe-tundra to open woodland ecosystems. Concurrent sedaDNA-inferred shifts in mammal communities, from mega-herbivore-dominated to mega-omnivores with smaller-bodied mammals, indicate collapse of the mammoth steppe ecosystem. Silhouette images illustrate the growth forms and representative mammalian taxa in each category, and are provided under the CC0 1.0 Universal license. Details on relative abundance calculations are provided in the Methods and Materials.

Robust reconstruction of millennial-scale ecological interactions and compositional dynamics from sedimentary ancient metagenomics

In total, 23,484,571 reads were used for terrestrial ecosystem reconstruction, corresponding to 16 mammalian and 50 seed-bearing plant families (data S1). These reads, with a best identity of ≥95% against the comprehensive taxonomic reference database (data S2), were retained as part of a multi-step strategy to minimize false positives and noise (Methods and Materials). The ancient origin of the reads was authenticated by read length distribution (fig. S1) and characteristic C-to-T substitutions at the 5' and 3' ends across taxa and time periods (fig. S2), with representative coverage of mammals and plants (fig. S3).

The sedaDNA-inferred composition changes (Fig. 1B) across four time transitions (T) that represent terrestrial ecosystem shifts in the Arctic (*7*, *15*, *17–19*). T1: a homogeneous steppe-tundra with abundant megaherbivores during the coldest and driest Last Glacial Maximum (25–20 ka), transitioning to herbaceous plants with megafauna still abundant, while woody plants began to advance during the cold and dry Late Glacial (20–15 ka); T2: rapid warming towards the early Holocene (15–10 ka), coinciding with a substantial increase in the abundance of woody plants while megaherbivores decline; T3: a transition from open landscapes to denser woody vegetation during the maximal Holocene warming phase (10–5 ka); and T4: re-expansion of herbaceous vegetation and the extinction of mammoths during the cooling of the Late Holocene (5–0 ka).

Based on these ecological transitions and addressing the fundamental challenge of inferring past ecological interactions from sedaDNA (*20*), we developed a comprehensive validation pipeline (detailed in Materials and Methods; see also fig. S4–11 and table S1–3) that establishes the reliability of ancient ecological network reconstruction.

Cascading effects: mammalian interactions shaped ecological turnover

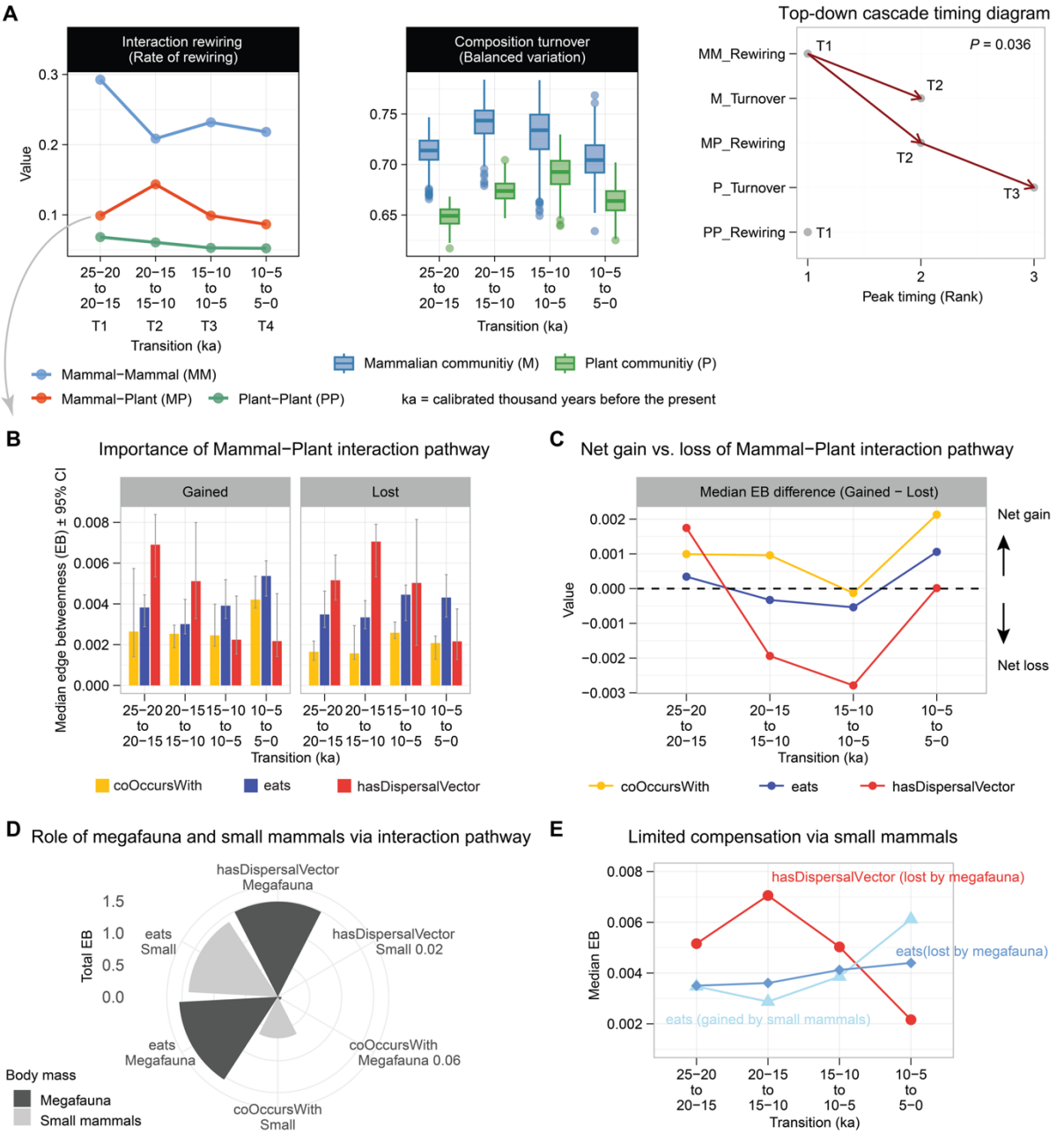

Fig 2. Cascading top-down regulation: mammal interaction dynamics drive ecological turnover over the past 25 ka. (**A**) Interaction rewiring (rate of rewiring) and composition turnover (balanced variation) reveal a top-down temporal cascade. (**B**) We measured mammal–plant interaction importance using edge betweenness (EB) across four time transitions. Interactions included seed dispersal (hasDispersalVector), trophic interactions (eats), and habitat co-occurrence (coOccursWith), using interaction pathways defined by the Global Biotic Interactions (GloBI) database. Each interaction was categorized by fate as gained or lost. The 95% confidence interval (CI) was calculated via bootstrap resampling with 1,000 replicates. (**C**) Net gain (positive) versus net loss (negative) of mammal–plant interactions across time. (**D**) Interaction pathway importance grouped by body mass highlights that megafauna (N = 8) primarily contribute to seed dispersal and trophic interactions, while small mammals (N = 8) are more involved in trophic interactions and habitat co-occurrence. Total EB values < 1 are displayed directly. Megafauna and smaller mammals are classified based on Bayesian regression estimates of body mass (estimated value > 0, fig. S9). (**E**) Small mammals gained trophic links with lower EB than those lost through megafaunal seed dispersal and trophic interactions until a partial compensation in the late Holocene (5–0 ka). Calculation and validation procedures are detailed in Materials and Methods and figs. S6, S7, S12–S17, and table S1–5.

Our reconstructed ecological networks, comprising mammal–mammal, mammal–plant, and plant–plant interactions, varied in both the number of taxa (nodes) and ecological

interactions (links) across the five time periods (table S4). We quantified and normalized interaction rewiring (i.e., changes in interactions among shared taxa), where a high rate of rewiring suggests rapid turnover in interaction structure, reflecting dynamic shifts in ecological roles or partner availability (*21*, *22*). We further quantified composition turnover (higher values indicate greater community heterogeneity) (*23*).

Our time-series sedaDNA data reveal a cascading effect of ecological change initiated by high mammal–mammal interaction rewiring (25–20 to 20–15 ka), followed by delayed peaks in mammalian composition and mammal–plant interaction rewiring (20–15 to 15–10 ka). Sequentially, mammal–plant interaction rewiring triggers maximum plant composition turnover (15–10 to 10–5 ka). We formally tested this cascade by comparing observed peaks by permutation testing. This revealed that the temporal sequence is significantly driven by mammalian interaction rewiring, which acts as an initial trigger (P = 0.036, one-side, 999 permutations, Fig. 2A).

We propose that the peak in mammalian interaction rewiring from 25–20 to 20–15 ka may reflect the ecological consequences of top predator loss (*24*). For instance, the extinction of large carnivores such as scimitar-tooth cats (*Homotherium serum*) in Eurasia around 24.7 ka (*18*), as a generalist predator of large herbivores in open landscapes (*25*), may have reduced predation pressure and enabled the expansion of megaherbivore populations. This is supported by our detection of a marked increase in relative abundance of megaherbivores (e.g., Elephantidae, Bovidae, Equidae, and Cervidae) from the Last Glacial Maximum (25–20 ka) to the late-glacial period (20–15 ka; Fig. 1B). This likely reshaped mammal–mammal interactions by altering competition and predation dynamics. Surviving megaherbivores and carnivores, with flexible diets (*25*), may have supported this rewiring. Their large ranges and mobility (fig. S8) enabled rapid reorganization of interactions across regions. We suggest that such flexibility, amplified by reduced top-down control, helped stabilize community composition, delaying turnover despite major shifts in interaction structure.

We detected a sharp decline in the relative abundance of megaherbivores, which coincided with a marked drop in mammalian interaction rewiring from 20–15 to 15–10 ka (Fig. 2A). A concurrent rise in network modularity (fig. S16) suggests that, rather than forming well-connected webs, surviving mammals increasingly clustered into more isolated groups with fewer cross-trophic interactions. Lower interaction redundancy made mammalian communities more vulnerable to perturbations, contributing to the pronounced turnover in composition during this transition. Thereafter, mammalian interaction rewiring remained low and compositional turnover declined into the late Holocene (5–0 ka), supporting the view that the decline in interaction redundancy and replacement capacity drove community simplification and reduced resilience (*13*).

Our sedaDNA records show no concurrent peak in plant compositional turnover with abundant megaherbivores from 25–20 to 20–15 ka. This finding suggests that trophic effects alone did not drive vegetation shifts, conflicting with the commonly held view that grazing necessarily causes strong vegetation change, such as herbivory reducing tree cover (*26*) or favoring grazing-tolerant grass and forbs (*27*, *28*). One plausible explanation for this discrepancy is that surveys conducted in already-defaunated ecosystems may be biased (*29*).

To explore this megafaunal grazing paradox, we measured edge betweenness centrality for mammal–plant interactions, which quantifies each link's importance in maintaining network connectivity as an indicator of ecosystem connectivity (*30*, *31*). We find that seed dispersal interactions (hasDispersalVector) exhibit the highest median edge betweenness (Fig. 2B) and the largest net gains (Fig. 2C) compared to trophic interactions (eats) and habitat co-occurrence (coOccursWith) during 25–20 ka and 20–15 ka. These seed dispersal interactions are primarily

associated with megafauna (Fig. 2D). These findings suggest that megafaunal-mediated seed dispersal served as a key integrative force, supporting ecological connectivity by enabling long-distance seed dispersal. This buffering capacity diminished significantly with the decline of megafauna from 15 ka onwards (Fig. 1B), leading to a dramatic loss of vital dispersal interactions (greatest net loss from 15–10 to 10–5 ka, Fig. 2C). This loss coincided with a peak in plant community turnover (Fig. 2A) and likely contributed to the collapse of the steppe-tundra biome. Although the other two interaction pathways and small mammals gained some prominence (Fig. 2C and E), they did not compensate functionally (see Supplementary Text for details).

Cumulatively, our findings reveal a previously overlooked mechanism: seed dispersal interactions played a pivotal role in buffering vegetation change, as long-distance megafaunal movement helped delay plant community turnover by millennia, even after mammalian community turnover had peaked.

Key mammal–plant interactions and their ecosystem-level influence

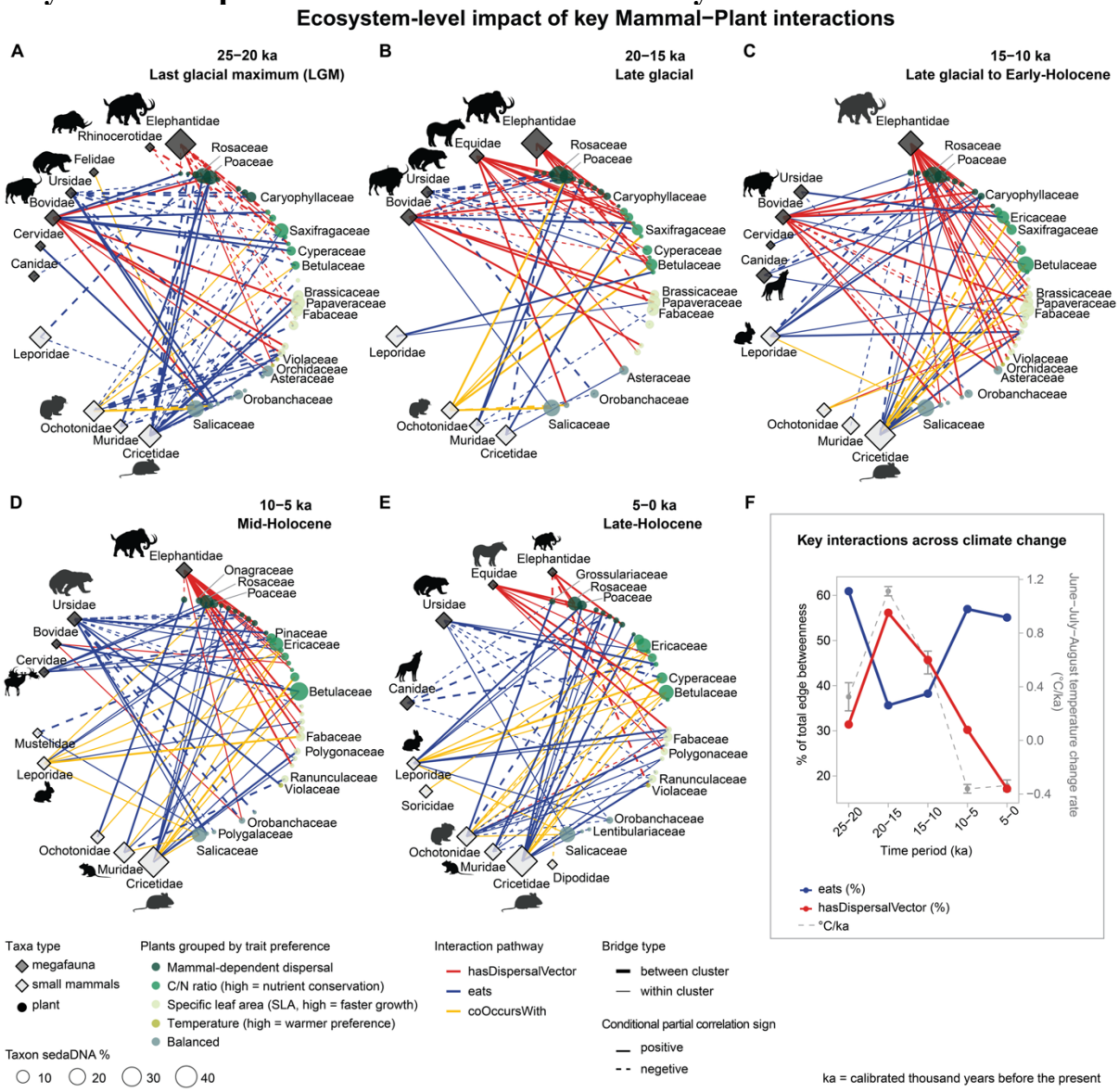

Fig. 3 Temporal dynamics of key mammal–plant interactions at ecosystem-level. (**A–E**) Key mammal–plant interactions over time. (**F**) The rate of summer (June–July–August) temperature change coincides with a shift in the dominant interaction pathway contributing to ecosystem connectivity, measured as the percentage of total edge betweenness (EB) of key interactions. Seed dispersal and trophic interactions are presented here. Node size reflects sedaDNA-based relative abundance; shapes distinguish megafauna, small mammals, and plants. Mammals are ordered by decreasing dispersal distance, plants by trait preferences. Link colors indicate interaction pathways; link borders indicate structural role within the network (within- vs. between-cluster bridges). Key interactions are defined as those with EB above the third quartile (Q3). Silhouette images are provided under the CC0 1.0 Universal license. Calculation procedures are detailed in Materials and Methods.

Beyond overall patterns, we focused on key mammal–plant interactions with EB above the third quartile (Q3) to determine which mammals regulate plant community structure and function, and through which interaction pathways, across time.

We find that key seed dispersal interactions are strongly associated with megaherbivores (e.g., Elephantidae, Bovidae, and Equidae) and are predominantly positive, except during the Last Glacial Maximum (Fig. 3A–E). This suggests they had a role as effective long-distance dispersers, maintaining ecological connectivity by linking otherwise distant or isolated taxa (*32*). In contrast, key trophic interactions involving mega-omnivores (e.g., Ursidae) are mainly negative (Fig. 3A–B and D–E), likely reflecting an extractive foraging strategy shaped by low

site fidelity and dietary opportunism (*33*). Unlike some herbivores with high spatial fidelity (e.g., Bovidae and Elephantidae) (*34*, *35*), Ursidae's highly mobile behavior likely led to intensive consumption in localized areas before moving on, probably imposing diffuse consumptive pressure across plant taxa with varying traits (*36*). This pattern of foraging may have limited opportunities for mutualistic interactions. Moreover, cervids, though also classified as megaherbivores, primarily contributed to positive trophic interactions. This likely reflects their relatively short dispersal distances and generalist herbivory (fig. S8), including browsing on nutrient-poor, high carbon-to-nitrogen (C/N) ratio plants such as Ericaceae (10–5 ka, Fig. 3D) and consumption of some fleshy fruits (e.g., Rosaceae during 15–5 ka, Fig. 3C and D). These patterns suggest cervids function more as localized consumers than landscape-scale seed vectors. These findings highlight that megafauna—even within herbivores—are functionally diverse.

The relative abundance of megaherbivores as key dispersers peaked around 20–15 ka, coinciding with the highest relative contribution of seed dispersal interactions to total edge betweenness (Fig. 3F), indicating strong ecosystem-level dispersal efficacy. Despite rapid climate warming during this period (Fig. 3F), plant compositional turnover remained low (Fig. 2A), suggesting that strong dispersal efficacy helped buffer vegetation change. However, these interactions gradually eroded afterwards: while still contributing more to connectivity than trophic interactions during 15–10 ka, their relative importance declined markedly and were eventually surpassed by trophic interactions during 10–5 ka and 5–0 ka, as the climate entered a more stable, warm phase. This progressive defaunation likely weakened overall ecosystem connectivity, limiting the ability of many plant species to colonize fragmented or newly available habitats. In turn, surviving mammals (e.g., cervids, ursids, and mustelids) increasingly relied on locally available vegetation, intensifying grazing and browsing pressure on a broader range of plant taxa (Fig. 3D).

Although key negative trophic interactions involving ursids were already present during the glacial periods (25–15 ka; Fig. 3A–C), their ecological impact was likely buffered by high mobility and the elevated importance of seed dispersal interactions (Fig. 3F) (*37*). However, ongoing defaunation reduced this buffering capacity, resulting in a sharp rise in both the relative importance and negativity of trophic interactions during 10–5 ka (Fig. 3D and F). By the late Holocene (5–0 ka), neither trophic nor seed dispersal interactions regained dominance (Fig. 3F), indicating a breakdown of previously dominant function roles and a shift towards loss of functional integrity and redundancy. This convergence, following the earlier decline of megaherbivores, suggests that low dispersal efficacy may have undermined the structural conditions necessary to sustain key trophic dynamics. As functional redundancy eroded, ecosystems became increasingly vulnerable, setting the stage for an extinction debt that likely manifested as progressive taxonomic and functional simplification during the late Holocene, relative to the megafauna-rich glacial ecosystems.

Surprisingly, facilitation of seed dispersal via mammal movement appears to be context-dependent. During the Last Glacial Maximum, many key dispersal links were negative (Fig. 3A). Our analysis shows that greater plant height tends to strengthen these negative associations (Effect size = –0.72 ± 0.32 SE, P = 0.037, table S6 and fig. S18–S19). This is likely because taller plants (e.g., Pinaceae) were mainly restricted to glacial refugia (*38*, *39*) and struggled to survive beyond them, making seed dispersal via mammal movement an ineffective colonization strategy. Instead, such interactions may have increased survival pressure on these taxa.

Interestingly, plants with higher leaf dry matter content (LDMC), a trait associated with slow-growing and stress-tolerant strategies, exhibit weaker negative associations (effect size =

0.52 ± 0.26 SE, $P = 0.056$; table S6). High LDMC, indicative of tougher, more durable leaves with greater structural investment, likely enhanced resilience to harsh environmental conditions, making mammal-mediated dispersal less detrimental. This trait-based advantage may explain the continued abundance of dwarf shrubs such as Ericaceae and Betulaceae, two families well known for stress tolerance, throughout the Last Glacial Maximum and into the late glacial period.

Functional traits determine turnover and resilience in mammal–plant mutualisms

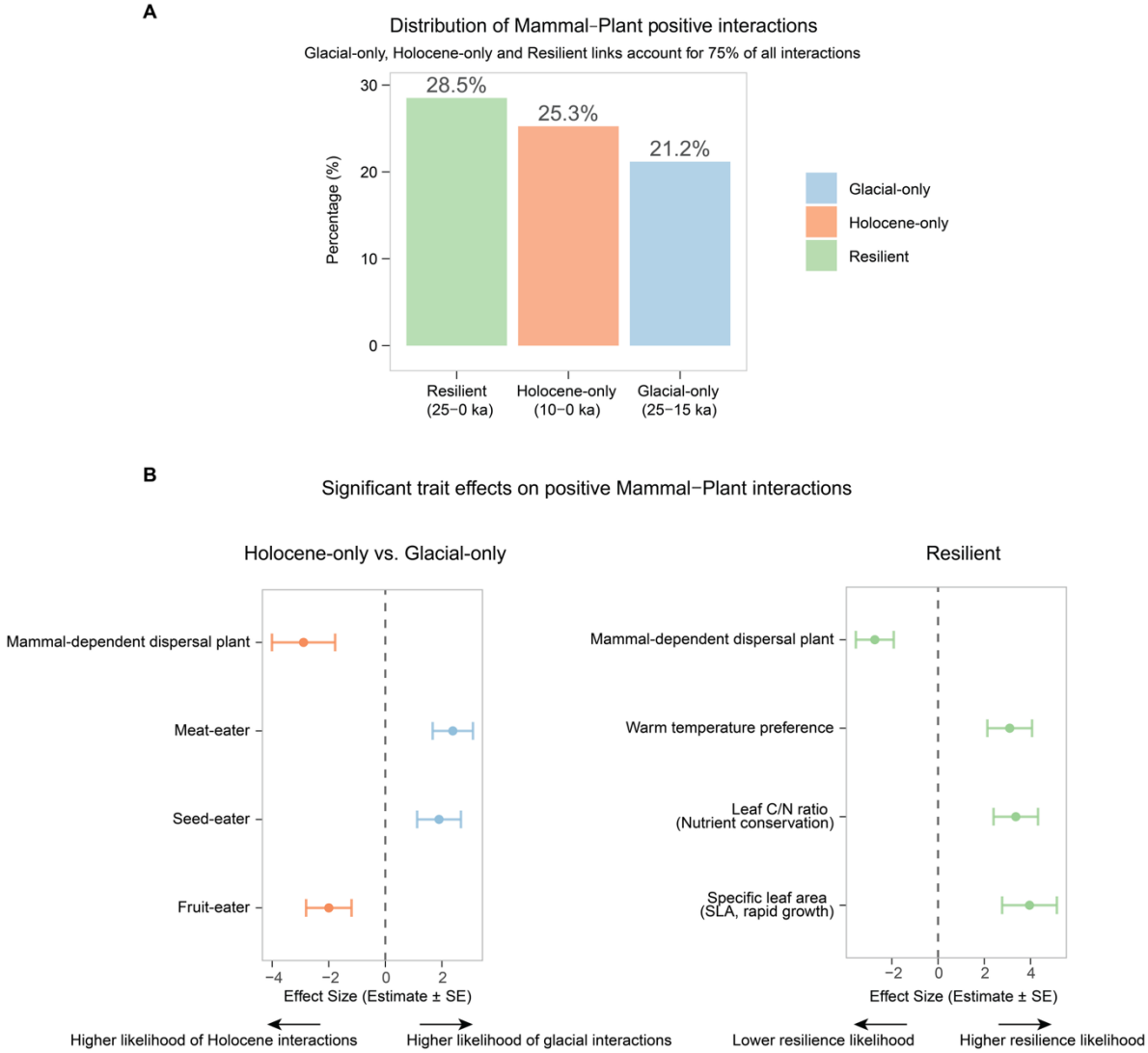

Fig. 4. Trait effects in mammal–plant positive interactions over the past 25 ka. (**A**) Classification of positive interactions into glacial-only, Holocene-only, and resilient categories. (**B**) Effects of traits on the likelihood of glacial-only, Holocene-only, and resilient positive interactions. Values represent generalized linear model (GLM) coefficients (effect size) ± standard errors (SE); only traits with significant effects ($P < 0.05$) are shown. Calculation and validation procedures are detailed in Materials and Methods and figs. S20–S21 and table S7–8.

Understanding which functional traits support persistent positive interactions can reveal the mechanisms that underpin long-term ecosystem resilience (*40*). We observe positive interactions, with 28.5% classified as resilient, 25.3% specific to the Holocene, and 21.2% specific to the glacial period (Fig. 4A). This pattern indicates that many glacial-period interactions were not reassembled under warmer Holocene conditions. The disappearance is associated with mammalian dietary specialization, with seed- and meat-eating mammals

showing a higher likelihood of glacial-specific interactions (Fig. 4B). This highlights the prevalence of positive associations involving omnivorous and granivorous taxa under resource-constrained conditions. In contrast, Holocene-specific positive interactions are more frequently associated with fruit-eating mammals and mammal-dependent dispersal plants (Fig. 4B). These findings reveal a fundamental ecological shift from mammal-benefiting commensalistic interactions during glacial periods to specialized mammal-plant mutualistic relationships in the Holocene.

During the glacial period, when megafaunal dispersers were abundant, plants likely faced minimal dispersal limitation and thus had little need to maintain stable, long-term associations permitting greater flexibility in partner switching. Meanwhile, omnivores (e.g., ursids) and granivores (e.g., sciurids) likely relied on plants as fallback or supplementary food sources, gaining benefits while offering little in return. Their foraging was opportunistic, and any seed dispersal that occurred was incidental rather than the result of close mutualistic relationships. Instead, the warmer and more stable conditions in the Holocene made long-distance dispersal particularly beneficial for plants, as it improved the likelihood of successful recruitment and range shifts for energy-intensive fruiting plants (*41*). Likewise, these conditions likely enabled plants to invest more in resource-demanding reproductive traits, such as fleshy fruits (*42*).

At the same time, reduced availability of dispersers intensified partner dependency in these mutualistic relationships. This was further exacerbated by weaker wind regimes compared to the glacial period (*43*), which limited the effectiveness of wind dispersal and increased reliance on mammal-mediated seed dispersal. As a result, remaining partnerships showed stronger reciprocal specialization, with plants increasing investment in fruit rewards to secure critical dispersal services. Thus, the loss of these commensalisms and mutualisms due to defaunation likely increased plant extinction that occurred during the early Holocene (*17*) and may have driven compositional turnover toward smaller seed sizes (fig. S22).

Resilient interactions are primarily associated with plant traits such as adaptation to temperature increases, higher leaf C/N ratios, and greater specific leaf area (Fig. 4B). These traits confer stress resistance, enable rapid growth in disturbed environments, and support adaptation to shifting climatic conditions.

Conclusions

Our time-series sedaDNA data offer novel evidence that rewiring of mammalian interactions triggered ecological cascades unfolding over millennia, ultimately contributing to the collapse of the Arctic mammoth-steppe. We identified that mammal-mediated seed dispersal was critical for maintaining ecosystem connectivity, but this role deteriorated as dispersers—particularly megaherbivores—were lost. These insights underscore the long-term, often delayed consequences of defaunation, implying that today's human-driven losses may likewise trigger ecological shifts that unfold far beyond the current century.

Our findings challenge the traditional perspective, which attributes the disappearance of the mammoth-steppe biome solely to climate warming that lead to vegetation change and, subsequently, to the loss of megafauna (*7*). Instead, our results highlight the active role of megafauna in shaping vegetation composition through long-distance seed dispersal, suggesting that restoring lost ecological functions via rewilding may support greater resilience under ongoing environmental change. Furthermore, we show that different megafauna contributed to ecosystem functioning via distinct interaction pathways with plants, highlighting that effective rewilding depends on restoring these ecological functions rather than merely reintroducing species.

Looking ahead, our findings suggest that interaction rewiring detected before major compositional shifts may serve as an early-warning signal of ecosystem reorganization. With finer temporal resolution, ancient metagenomic records could help identify subtle yet functionally significant changes, offering a quantitative framework to anticipate ecological tipping points.

REFERENCES AND NOTES

1. M. C. Urban, Accelerating extinction risk from climate change. Science 348, 571–573 (2015).

2. T. B. Atwood, S. A. Valentine, E. Hammill, D. J. McCauley, E. M. P. Madin, K. H. Beard, W. D. Pearse, Herbivores at the highest risk of extinction among mammals, birds, and reptiles. Sci. Adv. 6, eabb8458 (2020).

3. J. A. Estes, J. Terborgh, J. S. Brashares, M. E. Power, J. Berger, W. J. Bond, S. R. Carpenter, T. E. Essington, R. D. Holt, J. B. C. Jackson, R. J. Marquis, L. Oksanen, T. Oksanen, R. T. Paine, E. K. Pikitch, W. J. Ripple, S. A. Sandin, M. Scheffer, T. W. Schoener, J. B. Shurin, A. R. E. Sinclair, M. E. Soulé, R. Virtanen, D. A. Wardle, Trophic Downgrading of Planet Earth. Science 333, 301–306 (2011).

4. H. S. Rogers, I. Donoso, A. Traveset, E. C. Fricke, Cascading Impacts of Seed Disperser Loss on Plant Communities and Ecosystems. Annu. Rev. Ecol. Evol. Syst. 52, 641–666 (2021).

5. F. A. Smith, R. E. Elliott Smith, S. K. Lyons, J. L. Payne, Body size downgrading of mammals over the late Quaternary. Science 360, 310–313 (2018).

6. A. Cooper, C. Turney, K. A. Hughen, B. W. Brook, H. G. McDonald, C. J. A. Bradshaw, Abrupt warming events drove Late Pleistocene Holarctic megafaunal turnover. Science 349, 602–606 (2015).

7. Y. Wang, M. W. Pedersen, I. G. Alsos, B. De Sanctis, F. Racimo, A. Prohaska, E. Coissac, H. L. Owens, M. K. F. Merkel, A. Fernandez-Guerra, A. Rouillard, Y. Lammers, A. Alberti, F. Denoeud, D. Money, A. H. Ruter, H. McColl, N. K. Larsen, A. A. Cherezova, M. E. Edwards, G. B. Fedorov, J. Haile, L. Orlando, L. Vinner, T. S. Korneliussen, D. W. Beilman, A. A. Bjørk, J. Cao, C. Dockter, J. Esdale, G. Gusarova, K. K. Kjeldsen, J. Mangerud, J. T. Rasic, B. Skadhauge, J. I. Svendsen, A. Tikhonov, P. Wincker, Y. Xing, Y. Zhang, D. G. Froese, C. Rahbek, D. B. Nogues, P. B. Holden, N. R. Edwards, R. Durbin, D. J. Meltzer, K. H. Kjær, P. Möller, E. Willerslev, Late Quaternary dynamics of Arctic biota from ancient environmental genomics. Nature 600, 86–92 (2021).

8. M. M. Pires, The Restructuring of Ecological Networks by the Pleistocene Extinction. Annu. Rev. Earth Planet. Sci. 52, 133–158 (2024).

9. T. Poisot, D. B. Stouffer, D. Gravel, Beyond species: why ecological interaction networks vary through space and time. Oikos 124, 243–251 (2015).

10. M. M. Pires, M. Galetti, C. I. Donatti, M. A. Pizo, R. Dirzo, P. R. Guimarães, Reconstructing past ecological networks: the reconfiguration of seed-dispersal interactions after megafaunal extinction. Oecologia 175, 1247–1256 (2014).

11. A. B. Tóth, S. K. Lyons, W. A. Barr, A. K. Behrensmeyer, J. L. Blois, R. Bobe, M. Davis, A. Du, J. T. Eronen, J. T. Faith, D. Fraser, N. J. Gotelli, G. R. Graves, A. M. Jukar, J. H. Miller, S. Pineda-Munoz, L. C. Soul, A. Villaseñor, J. Alroy, Reorganization of surviving mammal communities after the end-Pleistocene megafaunal extinction. Science 365, 1305–1308 (2019).

12. C. P. Hedberg, S. K. Lyons, F. A. Smith, The hidden legacy of megafaunal extinction: Loss of functional diversity and resilience over the Late Quaternary at Hall's Cave. Glob. Ecol. Biogeogr. 31, 294–307 (2022).

13. F. A. Smith, E. A. Elliott Smith, A. Villaseñor, C. P. Tomé, S. K. Lyons, S. D. Newsome, Late Pleistocene megafauna extinction leads to missing pieces of ecological space in a North American mammal community. Proc. Natl. Acad. Sci. U.S.A. 119, e2115015119 (2022).

14. D. N. Morton, A. Keyes, A. K. Barner, L. E. Dee, Merging theory and experiments to predict and understand coextinctions. Trends Ecol. Evol. 37, 886–898 (2022).

15. G. M. MacDonald, D. W. Beilman, Y. V. Kuzmin, L. A. Orlova, K. V. Kremenetski, B. Shapiro, R. K. Wayne, B. Van Valkenburgh, Pattern of extinction of the woolly mammoth in Beringia. Nat. Commun. 3, 893 (2012).

16. M. Dehasque, P. Pečnerová, H. Muller, A. Tikhonov, P. Nikolskiy, V. I. Tsigankova, G. K. Danilov, D. Díez-del-Molino, S. Vartanyan, L. Dalén, A. M. Lister, Combining Bayesian age models and genetics to investigate population dynamics and extinction of the last mammoths in northern Siberia. Quat. Sci. Rev. 259, 106913 (2021).

17. J. Courtin, K. R. Stoof-Leichsenring, S. Lisovski, Y. Liu, I. G. Alsos, B. K. Biskaborn, B. Diekmann, M. Melles, B. Wagner, L. Pestryakova, J. Russell, Y. Huang, U. Herzschuh, Potential plant extinctions with the loss of the Pleistocene mammoth steppe. Nat. Commun. 16, 645 (2025).

18. A. J. Stuart, Late Quaternary megafaunal extinctions on the continents: a short review. Geol. J. 50, 338–363 (2015).

19. Y. Liu, S. Lisovski, J. Courtin, K. R. Stoof-Leichsenring, U. Herzschuh, Plant interactions associated with a directional shift in the richness range size relationship during the Glacial-Holocene transition in the Arctic. Nat. Commun. 16, 1128 (2025).

20. F. M. Callahan, J. K. Li, R. Nielsen, Challenges in Detecting Ecological Interactions Using Sedimentary Ancient DNA Data. Environ. DNA 7, e70067 (2025).

21. T. Poisot, E. Canard, D. Mouillot, N. Mouquet, D. Gravel, The dissimilarity of species interaction networks. Ecol. Lett. 15, 1353–1361 (2012).

22. T. Poisot, Dissimilarity of species interaction networks: quantifying the effect of turnover and rewiring. Peer Community J 2 (2022).

23. A. Baselga, Separating the two components of abundance-based dissimilarity: balanced changes in abundance vs. abundance gradients. Methods Ecol. Evol. 4, 552–557 (2013).

24. B. Van Valkenburgh, M. W. Hayward, W. J. Ripple, C. Meloro, V. L. Roth, The impact of large terrestrial carnivores on Pleistocene ecosystems. Proc. Natl. Acad. Sci. U.S.A. 113, 862–867 (2016).

25. D. G. Drucker, The Isotopic Ecology of the Mammoth Steppe. Annu. Rev. Earth Planet. Sci. 50, 395–418 (2022).

26. E. S. Bakker, J. L. Gill, C. N. Johnson, F. W. M. Vera, C. J. Sandom, G. P. Asner, J.-C. Svenning, Combining paleo-data and modern exclosure experiments to assess the impact of megafauna extinctions on woody vegetation. Proc. Natl. Acad. Sci. U.S.A. 113, 847–855 (2016).

27. S. E. Koerner, M. D. Smith, D. E. Burkepile, N. P. Hanan, M. L. Avolio, S. L. Collins, A. K. Knapp, N. P. Lemoine, E. J. Forrestel, S. Eby, D. I. Thompson, G. A. Aguado-Santacruz, J. P. Anderson, T. M. Anderson, A. Angassa, S. Bagchi, E. S. Bakker, G. Bastin, L. E. Baur, K. H. Beard, E. A. Beever, P. J. Bohlen, E. H. Boughton, D. Canestro, A. Cesa, E. Chaneton, J. Cheng, C. M. D'Antonio, C. Deleglise, F. Dembélé, J. Dorrough, D. J. Eldridge, B. Fernandez-Going, S. Fernández-Lugo, L. H. Fraser, B. Freedman, G. García-Salgado, J. R. Goheen, L. Guo, S. Husheer, M. Karembé, J. M. H. Knops, T. Kraaij, A. Kulmatiski, M.-M. Kytöviita, F. Lezama, G. Loucougaray, A. Loydi, D. G. Milchunas, S. J. Milton, J. W. Morgan, C. Moxham, K. C. Nehring, H. Olff, T. M. Palmer, S. Rebollo, C. Riginos, A. C. Risch, M. Rueda, M. Sankaran, T. Sasaki, K. A. Schoenecker, N. L. Schultz, M. Schütz, A. Schwabe, F. Siebert, C. Smit, K. A. Stahlheber, C. Storm, D. J. Strong, J. Su, Y. V. Tiruvaimozhi, C. Tyler, J. Val, M. L. Vandegehuchte, K. E. Veblen, L. T. Vermeire, D. Ward, J. Wu, T. P. Young, Q. Yu, T. J. Zelikova, Change in dominance determines herbivore effects on plant biodiversity. Nat. Ecol. Evol. 2, 1925–1932 (2018).

28. K. A. Bråthen, F. I. Pugnaire, R. D. Bardgett, The paradox of forbs in grasslands and the legacy of the mammoth steppe. Front. Ecol. Environ. 19, 584–592 (2021).

29. J.-C. Svenning, P. B. M. Pedersen, C. J. Donlan, R. Ejrnæs, S. Faurby, M. Galetti, D. M. Hansen, B. Sandel, C. J. Sandom, J. W. Terborgh, F. W. M. Vera, Science for a wilder Anthropocene: Synthesis and future directions for trophic rewilding research. Proc. Natl. Acad. Sci. U.S.A. 113, 898–906 (2016).

30. M. E. J. Newman, M. Girvan, Finding and evaluating community structure in networks. Phys. Rev. E 69, 026113 (2004).

31. R. Hashemi, H. Darabi, M. Hashemi, J. Wang, Graph theory in ecological network analysis: A systematic review for connectivity assessment. J. Clean. Prod. 472, 143504 (2024).

32. J. F. Brodie, A. Gonzalez, J. Mohd-Azlan, C. R. Nelson, G. Tabor, D. Vasudev, K. A. Zeller, R. J. Fletcher, A well-connected Earth: The science and conservation of organismal movement. Science 388, eadn2225 (2025).

33. M. A. Edwards, J. A. Nagy, A. E. Derocher, Low site fidelity and home range drift in a wide-ranging, large Arctic omnivore. Anim. Behav. 77, 23–28 (2009).

34. T. A. Morrison, J. A. Merkle, J. G. C. Hopcraft, E. O. Aikens, J. L. Beck, R. B. Boone, A. B. Courtemanch, S. P. Dwinnell, W. S. Fairbanks, B. Griffith, A. D. Middleton, K. L.

Monteith, B. Oates, L. Riotte-Lambert, H. Sawyer, K. T. Smith, J. A. Stabach, K. L. Taylor, M. J. Kauffman, Drivers of site fidelity in ungulates. J. Anim. Ecol. 90, 955–966 (2021).

35. R. Burton-Roberts, L. S. Cordes, R. Slotow, A. T. Vanak, M. Thaker, N. Govender, G. Shannon, Seasonal range fidelity of a megaherbivore in response to environmental change. Sci Rep 12, 22008 (2022).

36. S. S. Ogurtsov, The Diet of the Brown Bear (Ursus arctos) in the Central Forest Nature Reserve (West-European Russia), Based on Scat Analysis Data. Biol Bull Russ Acad Sci 45, 1039–1054 (2018).

37. D. García-Callejas, R. Molowny-Horas, M. B. Araújo, D. Gravel, Spatial trophic cascades in communities connected by dispersal and foraging. Ecology 100, e02820 (2019).

38. L. L. Anderson, F. S. Hu, D. M. Nelson, R. J. Petit, K. N. Paige, Ice-age endurance: DNA evidence of a white spruce refugium in Alaska. Proc. Natl. Acad. Sci. U.S.A. 103, 12447–12450 (2006).

39. L. Schulte, C. Li, S. Lisovski, U. Herzschuh, Forest-permafrost feedbacks and glacial refugia help explain the unequal distribution of larch across continents. J. Biogeogr. 49, 1825–1838 (2022).

40. S. Kéfi, C. J. Lortie, L. A. Cavieres, The importance of facilitative interactions in mediating climate change impact on biodiversity. Oikos 2024, e10984 (2024).

41. Y. Malhi, C. E. Doughty, M. Galetti, F. A. Smith, J.-C. Svenning, J. W. Terborgh, Megafauna and ecosystem function from the Pleistocene to the Anthropocene. Proc. Natl. Acad. Sci. U.S.A. 113, 838–846 (2016).

42. J. M. Alatalo, A. K. Jägerbrand, J. Dai, M. D. Mollazehi, A.-S. G. Abdel-Salam, R. Pandey, U. Molau, Effects of ambient climate and three warming treatments on fruit production in an alpine, subarctic meadow community. Am. J. Bot. 108, 411–422 (2021).

43. A. A. Velichko, N. Catto, A. N. Drenova, V. A. Klimanov, K. V. Kremenetski, V. P. Nechaev, Climate changes in East Europe and Siberia at the Late glacial–holocene transition. Quat. Int. 91, 75–99 (2002).

44. B. von Hippel, K. R. Stoof-Leichsenring, L. Schulte, P. Seeber, L. S. Epp, B. K. Biskaborn, B. Diekmann, M. Melles, L. Pestryakova, U. Herzschuh, Long-term fungus–plant covariation from multi-site sedimentary ancient DNA metabarcoding. Quat. Sci. Rev. 295, 107758 (2022).

45. J. Courtin, A. A. Andreev, E. Raschke, S. Bala, B. K. Biskaborn, S. Liu, H. Zimmermann, B. Diekmann, K. R. Stoof-Leichsenring, L. A. Pestryakova, U. Herzschuh, Vegetation Changes in Southeastern Siberia During the Late Pleistocene and the Holocene. Front. Ecol. Evol. 9 (2021).

46. W. Jia, B. K. Biskaborn, K. R. Stoof-Leichsenring, L. A. Pestryakova, U. Herzschuh, Vegetation and glacier dynamics are sensitive to summer (not winter) warming and the evidence for larch refugia in the 'Northern Pole of Cold' inferred from sedimentary ancient DNA and geochemistry. Quat. Sci. Rev. 331, 108650 (2024).

47. S. P. Thurston, Structure, petrology, and metamorphic history of the Nome Group blueschist terrane, Salmon Lake area, Seward Peninsula, Alaska. Geol. Soc. Am. Bull. 96, 600 (1985).

48. D. Walker, Vegetation Studies: Seward Peninsula 2000 (PDF)., version 1.0, UCAR/NCAR - Earth Observing Laboratory (2011); https://doi.org/10.5065/D6KS6PRJ.

49. S. Scheidt, R. Egli, M. Lenz, C. Rolf, K. Fabian, M. Melles, Mineral Magnetic Characterization of High-Latitude Sediments From Lake Levinson-Lessing, Siberia. Geophys. Res. Lett. 48, e2021GL093026 (2021).

50. S. A. Vyse, U. Herzschuh, A. A. Andreev, L. A. Pestryakova, B. Diekmann, S. J. Armitage, B. K. Biskaborn, Geochemical and sedimentological responses of arctic glacial Lake Ilirney, chukotka (far east Russia) to palaeoenvironmental change since ∼51.8 ka BP. Quat. Sci. Rev. 247, 106607 (2020).

51. S. Champlot, C. Berthelot, M. Pruvost, E. A. Bennett, T. Grange, E.-M. Geigl, An Efficient Multistrategy DNA Decontamination Procedure of PCR Reagents for Hypersensitive PCR Applications. PLOS ONE 5, e13042 (2010).

52. S. Liu, S. Kruse, D. Scherler, R. H. Ree, H. H. Zimmermann, K. R. Stoof-Leichsenring, L. S. Epp, S. Mischke, U. Herzschuh, Sedimentary ancient DNA reveals a threat of warming-induced alpine habitat loss to Tibetan Plateau plant diversity. Nat. Commun. 12, 2995 (2021).

53. M. T. Gansauge, T. Gerber, I. Glocke, P. Korlević, L. Lippik, S. Nagel, L. M. Riehl, A. Schmidt, M. Meyer, Single-stranded DNA library preparation from highly degraded DNA using T4 DNA ligase. Nucleic Acids Res. 45, e79–e79 (2017).

54. L. Schulte, N. Bernhardt, K. Stoof-Leichsenring, H. H. Zimmermann, L. A. Pestryakova, L. S. Epp, U. Herzschuh, Hybridization capture of larch (Larix Mill.) chloroplast genomes from sedimentary ancient DNA reveals past changes of Siberian forest. Mol. Ecol. Resour. 21, 801–815 (2021).

55. B. von Hippel, K. R. Stoof-Leichsenring, U. Çabuk, S. Liu, M. Melles, U. Herzschuh, Postglacial bioweathering, soil nutrient cycling, and podzolization from palaeometagenomics of plants, fungi, and bacteria. Sci. Adv. 11, eadj5527 (2025).

56. S. Chen, Y. Zhou, Y. Chen, J. Gu, fastp: an ultra-fast all-in-one FASTQ preprocessor. Bioinformatics 34, i884–i890 (2018).

57. S. Liu, K. R. Stoof-Leichsenring, L. Harms, L. Schulte, S. Mischke, S. Kruse, C. Zhang, U. Herzschuh, Tibetan terrestrial and aquatic ecosystems collapsed with cryosphere loss inferred from sedimentary ancient metagenomics. Sci. Adv. 10, eadn8490 (2024).

58. B. Langmead, S. L. Salzberg, Fast gapped-read alignment with Bowtie 2. Nat. Methods. 9, 357–359 (2012).

59. Y. Wang, T. S. Korneliussen, L. E. Holman, A. Manica, M. W. Pedersen, ngsLCA—A toolkit for fast and flexible lowest common ancestor inference and taxonomic profiling of metagenomic data. Methods Ecol. Evol. 13, 2699–2708 (2022).

60. C. Michelsen, A. Fernandez-Guerra, M. W. Pedersen, T. S. Korneliussen, metaDMG-dev/metaDMG-core: v0.37 metaDMG paper, Zenodo (2022); https://doi.org/10.5281/zenodo.7285167.

61. E. Palkopoulou, S. Mallick, P. Skoglund, J. Enk, N. Rohland, H. Li, A. Omrak, S. Vartanyan, H. Poinar, A. Götherström, D. Reich, L. Dalén, Complete Genomes Reveal Signatures of Demographic and Genetic Declines in the Woolly Mammoth. Curr. Biol. 25, 1395–1400 (2015).

62. S. Liu, M. V. Westbury, N. Dussex, K. J. Mitchell, M.-H. S. Sinding, P. D. Heintzman, D. A. Duchêne, J. D. Kapp, J. von Seth, H. Heiniger, F. Sánchez-Barreiro, A. Margaryan, R. André-Olsen, B. De Cahsan, G. Meng, C. Yang, L. Chen, T. van der Valk, Y. Moodley, K. Rookmaaker, M. W. Bruford, O. Ryder, C. Steiner, L. G. R. Bruins-van Sonsbeek, S. Vartanyan, C. Guo, A. Cooper, P. Kosintsev, I. Kirillova, A. M. Lister, T. Marques-Bonet, S. Gopalakrishnan, R. R. Dunn, E. D. Lorenzen, B. Shapiro, G. Zhang, P.-O. Antoine, L. Dalén, M. T. P. Gilbert, Ancient and modern genomes unravel the evolutionary history of the rhinoceros family. Cell 184, 4874-4885.e16 (2021).

63. A. P. Camargo, S. Nayfach, I.-M. A. Chen, K. Palaniappan, A. Ratner, K. Chu, S. J. Ritter, T. B. K. Reddy, S. Mukherjee, F. Schulz, L. Call, R. Y. Neches, T. Woyke, N. N. Ivanova, E. A. Eloe-Fadrosh, N. C. Kyrpides, S. Roux, IMG/VR v4: an expanded database of uncultivated virus genomes within a framework of extensive functional, taxonomic, and ecological metadata. Nucleic Acids Res. 51, D733–D743 (2023).

Acknowledgments

We used ChatGPT to improve language readability and clarity. All AI-generated outputs were carefully reviewed and edited by the authors. We thank C. Böckel for formatting the IMG/VR v4 virus reference database, C. Jenks for English proofreading, and J. Klimke for assistance with genetic laboratory work.

Funding

European Research Council (ERC, Glacial Legacy, grant no. 772852 to U.H.)

Deutsche Forschungsgemeinschaft (DFG, German Research Foundation) Gottfried Wilhelm Leibniz Award (grant no. HE 2622/34-1 to U.H.)

Deutsche Forschungsgemeinschaft (DFG, grants no. 514539694 to U.H.)

United States National Science Foundation (U.S. NSF, grant no. 2303462 to D.S.K.)

Bundesministerium für Bildung und Forschung (BMBF, German Federal Ministry for Education and Research, grant no. 03G0859A to M.M.).

Author contributions

Conceptualization: S.L., U.H.

Methodology: S.L., K.R.S., U.H.

Validation: S.L., K.R.S, D.S.K.

Formal analysis: S.L

Investigation: K.R.S., W.J., D.S.K., S.L., U.H., B.K.B., B.D., H.M., M.M., L.A.P.

Resources: U.H., B.D., M.M., D.S.K.

Data curation: S.L., K.R.S., D.S.K., U.H.

Writing – original draft: S.L.

Writing – review & editing: S.L., U.H., M.T.H., D.S.K., K.R.S., B.K.B., M.M., B.D., W.J, H.M., L.A.P.

Visualization: S.L.

Supervision: U.H., S.L.

Project administration: U.H., S.L., K.R.S.

Funding acquisition: U.H., D.S.K., M.M.

Competing interests

Authors declare that they have no competing interests.

Data and materials availability

For transparency and reproducibility, source data and code are provided in supplementary materials and/or deposited in open access repositories. Specifically, raw metagenomic (shotgun sequencing) data is available in the European Nucleotide Archive (ENA) under BioProject accessions PRJEB94536 (Lake Levinson Lessing), PRJEB80635 (Lake Ilirney), PRJEB80642 (Lake Bolshoe Toko), PRJEB82635 (Lake Ulu), and PRJEB82717 (Lake Salmon). Raw metagenomic data for Lake Lama was previously published and is available in the ENA under BioProject accession PRJEB80877 (*44*). The scripts implementing the bioinformatic workflows, taxonomic reference indexing, taxonomic classification, and ancient DNA damage analysis, as well as an example tutorial illustrating taxonomic classification data, are archived on Zenodo (https://zenodo.org/records/17974857), with the actively maintained source code available on GitHub (https://github.com/sisiliu-research/EnviHoli).

Materials and Methods

Sites settings

The six lake sediment cores investigated span the Pleistocene–Holocene transition and are located across Siberia and Alaska, encompassing the Beringia region (Fig. 1A). This spatial distribution enables the investigation of mammalian and vegetation changes across areas formerly occupied by the Pleistocene mammoth-steppe.

The geophysical and vegetation characteristics of the catchments and surrounding areas of Lakes Levinson Lessing (74.47°N, 98.67°E; 48 m a.s.l.), Lama (69.53°N, 90.20°E; 53 m a.s.l.), Ilirney (67.35°N, 168.32°E; 1790 m a.s.l.), Ulu (63.34°N, 141.04°E; 950 m a.s.l.), and Bolshoe Toko (56.25°N, 130.50°E; 903 m a.s.l.) have been previously described in detail (*17*, *44–46*). In summary, these sites span a broad range of geological settings across western Russia and eastern Siberia, from rims of the Putorana Plateau (Lake Lama) and the Byrranga Mountains of the Taymyr Peninsula (Lake Levinson Lessing) to the Stanovoy Mountain Range (Lake Bolshoe Toko), Oymyakon Upland (Lake Ulu), and Chukotka near the Anadyr Mountains (Lake Ilirney). All sites experience a strongly continental climate, with mean January temperatures ranging from −65°C to −28.8°C and mean July temperatures between 12.1°C and 34°C. Bedrock geology is generally dominated by crystalline and metamorphic units, including granite, gneiss, and schist, while vegetation ranges from sparse typical tundra to *Larix*-dominated taiga.

Lake Salmon (64.91°N, 164.99°W; 208 m a.s.l.) is a glacially formed lake situated south of the Kigluaik Mountains, about 47 km north-northeast of Nome, Alaska. The lake covers 7.5 km², reaches a maximum depth of 21.6 m, and has a catchment area of 215 km². The catchment is primarily underlain by silicate-rich, high- to medium-grade metamorphic rocks of the Nome Group, including amphibolite- and granulite-facies of gneiss and biotite schist (*47*). Mean January and July temperatures are −14.6 °C and 10.5 °C, respectively, based on records from meteorological station Nome (49 km away, 11 m a.s.l.). The modern vegetation consists of dwarf to tall shrub tundra and dry-to-moist tundra communities, dominated by species such as *Alnus crispa*, *Calamagrostis canadensis*, *Spiraea beauverdiana*, *Senecio lugens*, *Betula nana*, *Loiseleuria procumbens*, *Stereocaulon paschale*, and *Rhododendron camtschaticum* (*48*).

Cores, chronologies, and sedaDNA materials

Core collection, radiocarbon dating, and age–depth models have been previously described for Lakes Levinson Lessing (core ID: Co1401) (*49*), Lama (PG1341) (*44*), Ilirney (EN18208) (*50*), Ulu (EN21103) (*46*), and Bolshoe Toko (PG2133) (*45*).

In July 2022, a 17.5-m sediment core (EN22502) was retrieved from Salmon Lake at a water depth of 21.6 m using a UWITEC Niederreiter 90 mm piston corer. After coring, the sediment was sealed in sterile plastic liners and transported to the Alfred Wegener Institute, Helmholtz Centre for Polar and Marine Research (AWI) in Potsdam, where it was stored in the dark at 4 °C prior to sampling and analysis. Core opening and subsampling were conducted in a dedicated climate chamber (10 °C) at the GFZ Helmholtz Centre for Geosciences in Potsdam, a facility where no molecular genetic work is performed. All cleaning procedures followed established protocols to avoid cross-contamination from modern DNA and between sediment samples (*51*). To reduce contamination risk, about 3 mm of the exposed core surface was removed using a sterile, single-use blade. Only the inner sediments were stored in 8 mL sterile tubes at −20 °C until DNA extraction.

The age–depth model of Lake Salmon core EN22502 is based on accelerator mass spectrometry (AMS) radiocarbon dating of 49 macrofossil samples conducted at the Arizona Climate and Ecosystems (ACE) Isotope Laboratory, Northern Arizona University.

Radiocarbon ages were calibrated to calendar years before present (BP, where present = AD 1950) using CALIB v8.2. The complete dataset and age–depth model have been deposited in PANGAEA (identifier PDI-41918).

DNA extraction, library preparation and shotgun sequencing

Molecular genetic analyses of sediment samples were carried out in the dedicated palaeogenetic laboratories at AWI, Potsdam, Germany. DNA was extracted from all lake sediment cores following a uniform protocol established for the study (*17*, *44–46*). In brief, each DNA extraction batch included nine sediment samples and one extraction control. Extractions followed a partially modified protocol of the PowerMax® Soil DNA Isolation Kit (Mo Bio Laboratories, Inc., USA) (*52*). The initial DNA concentration of the sedimentary ancient DNA (sedaDNA) isolates and blanks was measured using 1 µL of extract with the dsDNA BR Assay and Qubit® 2.0 fluorometer (Invitrogen, USA). Extracts were then concentrated and purified using the GeneJET PCR Purification Kit (Thermo Fisher Scientific Inc., USA), followed by a second concentration measurement. All purified sedaDNA isolates and blanks were diluted to 3 ng/µL, aliquoted into 15 µL portions to avoid repeated freeze–thaw cycles, and stored at −20 °C as working stocks for library preparation.

DNA libraries for all six sediment cores were prepared using a single-stranded DNA library protocol (*53*), including the second adapter ligation (CL53/CL72) performed on a thermomixer (*54*). Full details are described for Lake Lama (*55*) and were followed for other five cores. In this study, 29 (Levinson Lessing), 17 (Ilirney), 24 (Ulu), 27 (Bolshoe Toko), and 29 (Salmon Lake) sedaDNA isolates were processed for library preparation. Each library batch included 30 ng of DNA extract, at least one extraction blank, and one library blank. All libraries were quantified using quantitative polymerase chain reaction (qPCR), indexed with P5 (01–06, 11, 15–18, 46, 51, 64, 67, 72) and P7 primers (20, 21, 26, 27, 29, 40, 57, 60, 65, 82, 88, 91–96), purified using the MinElute PCR Purification Kit (Qiagen, Germany), and initially quality-checked on the 4200 TapeStation system (Agilent, G2991AA). Library-specific sequencing information is summarized in Data S3. In total, 170 sedaDNA samples (including 44 previously published shotgun-sequenced samples from Lake Lama (*55*), dated back to 58.2 ka) and 64 controls were processed for bioinformatic analysis.

Bioinformatic analyses

We assessed the quality of raw reads (10,058,696,099) using FastQC (v0.7.11) and performed two-step deduplication to improve confidence in the uniqueness of recovered reads: first with clumpify.sh (BBMap v0.20.1, dedupe=t), followed by dedupe.sh from BBTools (https://archive.jgi.doe.gov/data-and-tools/software-tools/bbtools/) to further remove redundant read pairs. Adapter trimming and merging of paired-end reads were conducted using fastp (v0.11.9) (*56*), with quality, complexity, length filters, polyG tail trimming, and polyX tail trimming applied as described in (*57*).

We performed taxonomic classification on merged reads (5,609,140,389) via end-to-end alignment with Bowtie2 (v2.5.1) (*58*). Classification was conducted using ngsLCA (*59*), as implemented in MetaDMG (v0.37) (*60*), which subsequently assessed postmortem damage patterns to evaluate the ancient origin of the classified taxa. To improve accuracy and sensitivity of taxonomic classification, we established a curated reference database (Data S2) incorporating all available RefSeq genomes from National Center for Biotechnology Information (NCBI, as of August 14, 2023), the full NCBI nucleotide (NT) database (as of September 19, 2022), chloroplast and mitochondria genomes of plant species occurring in SibAla region [as defined in ref (*17*)], mitochondrial genomes of mammals from the SibAla region, chloroplast genomes of *Abies sibirica* (NC_035067.1) and *Pinus pumila* (NC_041108.1), genomes of extinct mammals [*Mammuthus primigenius*, TaxID: 37349, (*61*); *Coelodonta antiquitatis*, TaxID: 222863, (*62*)], PhyloNorway (*7*), and viral genomes from

683 IMG/VR v4 (*63*). The reference index was built using Bowtie2 (v2.5.1) with default settings
684 (*58*). Merged reads were aligned against this indexed reference with up to 1000 valid and
685 unique alignments per read (-k 1000). Resulting candidates were then sorted and taxonomically
686 classified using ngsLCA with a minimum identity threshold of 95% (*59*). Classified read counts
687 for each sediment sample and control are summarized in Data S3. All controls yielded read
688 counts several orders of magnitude lower than sediment samples, suggesting no evidence of
689 cross-sample contamination.